Am J Transl Res 2026;18(4):3085-3096
www.ajtr.org /ISSN:1943-8141/AJTR0172092

Original Article

Application of magnetic resonance diffusion tensor imaging for the treatment of hemifacial spasm

Yupeng Guo[1,2], Xuanwei Dong[2], Min Liu[2], Fangang Meng[1,3,4]

[1]Beijing Neurosurgical Institute, Beijing Tiantan Hospital, Capital Medical University, Beijing 100070, China; [2]Department of Neurosurgery, Aviation General Hospital, Beijing 100012, China; [3]Beijing Key Laboratory of Neurostimulation, Beijing 100070, China; [4]Chinese Institute for Brain Research, Beijing 102206, China

Received February 12, 2026; Accepted March 14, 2026; Epub April 15, 2026; Published April 30, 2026

Abstract: Objectives: To evaluate diffusion tensor imaging (DTI) for assessing facial nerve root exit zone (REZ) microstructure in hemifacial spasm (HFS) and predicting microvascular decompression (MVD) outcomes. Methods: Data from 60 patients with primary unilateral HFS and 30 healthy volunteers were retrospectively examined. High-resolution 3.0T DTI was performed on all participants. DTI data (b=1000 s/mm^2, 32 directions) were processed using FMRIB Software Library. The fractional anisotropy (FA), mean diffusivity (MD), axial diffusivity (AD), and radial diffusivity (RD) were derived from the facial nerve REZ. Group comparisons and receiver operating characteristic curve analysis assessed diagnostic performance. Preoperative DTI parameters were also evaluated for predicting MVD outcomes. Results: In HFS, FA on the symptomatic side (0.35±0.06) was significantly lower than that on the contralateral side (0.48±0.05) and controls (0.49±0.04, P<0.001). MD and RD were significantly elevated (both P<0.001), while AD remained stable. The area under the curve (AUC) for FA in diagnosing HFS was 0.968 (sensitivity 86.00%, specificity 98.00%). Multivariate logistic regression analysis showed that the preoperative FA value was an independent predictor of postoperative outcomes (odds ratio=0.752, P=0.005), and the optimal cutoff value for FA was ≤ 0.378 (AUC=0.780). Conclusions: DTI noninvasively quantifies facial nerve REZ microstructural damage in HFS, characterized by reduced FA and elevated RD. As diagnostic and prognostic biomarkers, FA differentiates pathological compression from asymptomatic contact, supporting clinical decisions.

Keywords: Hemifacial spasm, diffusion tensor imaging, microvascular decompression, neurovascular compression, prognosis prediction

Introduction

Hemifacial spasm (HFS) is a common cranial nerve dysfunction disorder, which is characterized by paroxysmal and involuntary twitching of the facial muscles on one side. Its pathophysiologic mechanism is closely related to pulsatile compression of the facial nerve root exit zone (REZ) [1, 2]. Epidemiological data show that the incidence of HFS is about 0.78 per 100,000 person-years. It is more common in Asian populations, slightly more frequent in females than in males, and often occurs in middle-aged and older adults (40-60 years) [3]. Although not life-threatening, long-term involuntary facial twitching can lead to social withdrawal, anxiety, depression, and reduced professional functioning, all of which significantly affect patients' quality of life [4-6].

Microvascular decompression (MVD) is the established surgical treatment for HFS, but some patients experience poor outcomes or recurrence after surgery [7], highlighting the limitations of the preoperative evaluation system. At present, clinical methods to assist MVD decision-making mainly include high-resolution magnetic resonance imaging (MRI) to visualize neurovascular contact (NVC), neurophysiological monitoring (e.g., abnormal muscle response) to help localize offending vessels, and intraoperative neuronavigation [8, 9]. However, the above methods are all based on "morphology" or "electrophysiological phenomena" and cannot directly quantify microstructural damage to the nerve tissue itself, making it difficult to predict an individual's surgical prognosis. Although conventional high-resolution MRI (e.g., 3D-T2 and 3D-TOF-MRA) can clearly show the

https://doi.org/10.62347/CXKE9639

morphologic characteristics of NVC [10, 11], it cannot distinguish pathological compression from asymptomatic contact. Asymptomatic NVC is common in healthy individuals, with its prevalence rising with age [12]. This means that the presence of "contact" on imaging alone does not constitute a surgical indication, and excessive reliance on morphologic criteria may lead to unnecessary exploration or missed diagnosis [13]. In addition, conventional MRI cannot quantify microstructural changes after nerve compression, such as demyelination, axonal injury, or gliosis [14, 15]. Diffusion tensor imaging (DTI) measures water molecule diffusion anisotropy using diffusion-sensitizing gradients, which indirectly reflects the integrity, myelination, and organization of white matter fiber tracts. DTI parameters-including fractional anisotropy (FA), mean diffusivity (MD), axial diffusivity (AD) and radial diffusivity (RD) - have well-established biophysical correlates. FA quantifies the degree of diffusion anisotropy, which reflects fiber density and organizational coherence. MD reflects the overall diffusion capacity. AD and RD are sensitive to axon and myelin integrity, respectively [16-19]. In recent years, DTI has been increasingly applied to evaluate nerve microstructure in cranial nerve disorders such as trigeminal neuralgia (TN) and vestibular schwannoma, showing its ability to quantify tissue damage [20, 21]. However, when imaging small cranial nerves such as the facial nerve in the brainstem region, DTI faces technical challenges-including magnetic field inhomogeneity and small nerve caliber-that require sequence optimization and localized scanning strategies [22]. Worldwide, few studies have systematically investigated facial nerve REZ DTI metrics in HFS, with particularly scarce data correlating them with MVD outcomes.

Accordingly, this study evaluates DTI for HFS diagnosis and therapeutic guidance. First, an established standardized protocol for DTI data acquisition and post-processing was used to extract microstructural metrics of the facial nerve REZ. Second, this retrospective study quantified alterations in DTI metrics at the REZ in HFS and compared their diagnostic performance with that of conventional MRI. Finally, based on postoperative follow-up data, the predictive value of preoperative DTI metrics for long-term MVD outcomes was evaluated. Through multimodal image fusion and blinded analysis, this study assessed DTI as an objective imaging biomarker to support evidence-based, precision management of HFS using real-world data.

Materials and methods

Study design

Approval for this retrospective study was granted by the Aviation General Hospital Institutional Review Board (Approval No.: HK2025-108). The ethics committee waived informed consent due to the retrospective use of anonymized data. The study strictly adhered to the ethical standards of the Declaration of Helsinki and the International Code of Medical Ethics. From January 2020 to June 2025, the neurosurgical outpatient department of our hospital consecutively recruited 60 patients with primary unilateral hemifacial spasm (HFS group) and 30 age- and sex-matched healthy volunteers (healthy control group, HC group). All participants underwent 3.0T MRI at our institution. This analysis used archived imaging data and electronic medical records. Image post-processing and parameter extraction followed standardized protocols. The study workflow is illustrated in **Figure 1**.

Subjects

HFS group: Sixty patients with primary unilateral HFS were retrospectively enrolled, including 33 with left-sided and 27 with right-sided involvement.

Inclusion criteria: ① Meeting the internationally recognized clinical diagnostic criteria for HFS: paroxysmal involuntary twitching of the facial muscles on one side, usually starting in the orbicularis oculi muscle and gradually extending downward; ② Symptoms have lasted for more than 6 months, with poor response to drug therapy (e.g., carbamazepine, oxcarbazepine) or intolerable side effects; ③ Age between 18 and 70 years.

Exclusion criteria: ① Secondary HFS (e.g., posterior fossa tumors, vascular malformations); ② Bilateral HFS or concomitant movement disorders; ③ History of ipsilateral surgery or trauma; ④ Contraindications to MRI examination; ⑤ Severe organ dysfunction or mental illness; ⑥ Image quality insufficient for analysis.

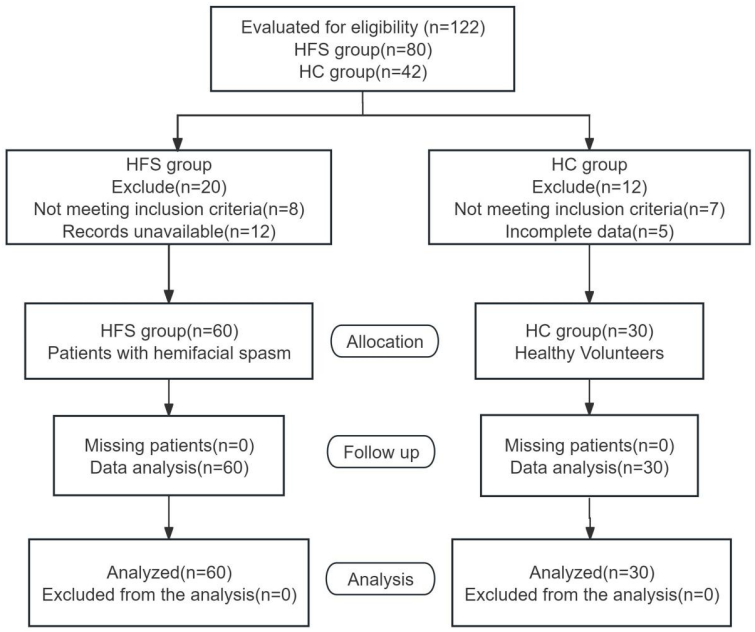

Figure 1. Design flow chart. Note: HFS: hemifacial spasm; HC: healthy control.

HC group: Thirty age- and sex-matched healthy volunteers without HFS were retrospectively enrolled. All subjects had no intracranial abnormalities, as confirmed by neurological examination and brain MRI.

Acquisition and processing of imaging data

Data collection: (1) Structural imaging included 3D-CISS/3D-FIESTA and 3D-TOF-MRA sequences. The parameters were set as follows: repetition time 1200 ms, echo time 120 ms for 3D-T2; and repetition time 23 ms, echo time 3.5 ms for 3D-TOF-MRA. The slice thickness was 0.8 mm, and the neurovascular anatomy of the cerebellopontine angle area was displayed with high contrast. (2) DTI: A SS-SE-EPI sequence was used. The optimized parameters included a b-value of 1000 s/mm^2, 32 diffusion-sensitive gradient directions, 2 mm isotropic voxels, and parallel imaging (acceleration factor of 2) to reduce distortion.

Data processing and analysis: (1) DTI preprocessing: Preprocessing (format conversion, eddy current and motion correction, skull stripping), tensor fitting, and parametric mapping (FA, MD, AD, RD) were performed using FMRIB Software Library v6.0. (2) Region of interest (ROI) analysis: Rigid registration was used to align DTI maps with high-resolution 3D-T2 images. Two blinded neuroradiologists independently delineated the facial nerve REZ (the first 3 mm segment after the nerve exits the brainstem), and the average DTI parameters were extracted. Inter-rater reliability was assessed using the intraclass correlation coefficient (ICC), with an ICC >0.8 considered acceptable. (3) Conventional MRI evaluation: Fusion images from 3D-T2 and 3D-TOF-MRA were blindly evaluated by senior neurosurgeons to determine the presence of NVC and the degree of compression (grade I-III).

Clinical follow-up review: We retrospectively obtained 6 month postoperative follow-up data from HFS patients who underwent MVD. Surgical outcomes were evaluated using the international efficacy grading standard (grade I-IV).

Outcome measures

The main outcome measures of this study comprised multidimensional assessments, including: (1) DTI metrics: FA, MD, AD, and RD values of the facial nerve REZ; (2) The ability of DTI to distinguish pathologic compression from asymptomatic contact, assessed by comparing DTI metrics on the asymptomatic NVC side in the HC group; (3) Postoperative outcomes at 12 months after MVD (classified as good or poor prognosis); (4) Correlation between DTI metrics and disease duration and spasm severity (Cohen grade).

Sample size calculation

Sample size was determined to detect FA differences at the REZ between HFS patients and controls. According to the preliminary results of our research group and previous literature [23], symptomatic-side FA in HFS was approximately 0.35±0.06, and the average FA value in the HC group (averaged across both sides) was about 0.49±0.04. With α=0.05, 1-β=0.90, and a two-sample *t*-test, PASS 15.0 estimated a minimum of 12 subjects per group. Allowing for 10-15% missing data in this retrospective design, en-

Table 1. Participant characteristics at baseline

Characteristic	HFS group (n=60)	HC group (n=30)	χ^2/t	*P*
Age (years)	52.11±8.54	51.91±9.52	0.101	0.920
Sex (M/F)	26/34	12/18	0.091	0.763
Hypertension, n (%)	18 (30.0)	7 (23.3)	0.461	0.497
Diabetes, n (%)	7 (11.7)	2 (6.7)	0.553	0.457
Affected side (L/R)	33/27	-	-	-
Mean disease duration (years)	5.35±2.68	-	-	-
Spasm severity (Cohen grade)	2.81±0.79	-	-	-

Note: HFS: hemifacial spasm; HC: healthy control; M/F: male/female; L/R: left/right.

rollment targets were set at ≥50 HFS patients and ≥25 controls. Final enrollment comprised 60 HFS patients and 30 controls, satisfying all statistical criteria.

Statistical analysis

SPSS 25.0 and R language were used for statistical analysis. Normality of continuous variables was assessed using the Shapiro-Wilk test. Normally distributed variables are presented as mean ± standard deviation, while non-normally distributed variables are presented as median with interquartile range. For comparisons between two groups, independent-sample Student's t-test was used for normally distributed data, and the Mann-Whitney U test was applied for non-normally distributed data. For comparisons among multiple groups, one-way analysis of variance was performed, followed by least significant difference post-hoc test for pairwise comparisons when the overall F-test was significant. Categorical variables were compared using the chi-square (χ^2) test or Fisher's exact test, as appropriate. Receiver operating characteristic curve analysis was conducted to evaluate the diagnostic performance of DTI metrics (FA, MD, RD). The area under the curve (AUC) with 95% confidence interval (CI) was calculated for each metric. The optimal cutoff value was determined by maximizing the Youden index (sensitivity + specificity - 1). Sensitivity, specificity, positive predictive value, and negative predictive value were reported. Correlations between DTI parameters and clinical variables (disease duration, spasm severity) were assessed using Pearson correlation coefficient for normally distributed data or Spearman's rank correlation coefficient for non-normally distributed data. To identify independent predictors of postoperative outcome, univariate logistic regression was first performed to screen variables with $P<0.10$. Variables meeting this threshold were entered into a multivariate binary logistic regression model. Due to the small number of events (n=5) in the poor prognosis group, Firth's penalized likelihood method was applied to reduce potential small-sample bias. Model fit was assessed using the Hosmer-Lemeshow goodness-of-fit test. The stability of estimates was evaluated by bootstrap resampling with 1,000 replicates to generate bias-corrected 95% CIs. All statistical tests were two-tailed, and statistical significance was defined as $P<0.05$.

Results

Baseline characteristics and conventional MRI findings

A total of 60 patients with primary unilateral HFS group and 30 age- and sex-matched HC group were enrolled in this study. As shown in **Table 1**, there were no significant differences in baseline data such as age, gender, or prevalence of hypertension and diabetes between the two groups ($P>0.05$), showing good comparability. In the HFS group, the average course of disease was 5.35±2.68 years, and the average Cohen score was 2.81±0.79. The left side was involved in 33 cases and the right side in 27 cases.

The two reviewers showed good agreement on the presence of NVC (kappa=0.85). Among the 60 patients with HFS, conventional MRI detected definite NVC on the affected side in 58 patients (96.67%), yielding a concordance rate of 96.67% with surgical findings (all 60 patients had offending vessels). The offending vessels were primarily the anterior inferior cerebellar artery (40 patients, 66.67%), followed by the posterior inferior cerebellar artery (12

Table 2. Intergroup and interside comparisons of DTI metrics at the facial nerve REZ

Group/Side	FA	MD (×10^{-3} mm^2/s)	RD (×10^{-3} mm^2/s)	AD (×10^{-3} mm^2/s)
HFS group (n=60)				
Affected side	0.35±0.06	1.25±0.15	0.95±0.14	1.45±0.18
Unaffected side	0.48±0.05	1.05±0.10	0.78±0.09	1.42±0.15
HC group (n=30)				
Bilateral mean	0.49±0.04	1.03±0.09	0.76±0.08	1.43±0.14
P-value				
Affected vs. Unaffected (HFS)	<0.001	<0.001	<0.001	0.323
Affected (HFS) vs. HC group	<0.001	<0.001	<0.001	0.596
Unaffected (HFS) vs. HC group	0.343	0.358	0.306	0.761

Note: FA: fractional anisotropy; MD: mean diffusivity; RD: radial diffusivity; AD: axial diffusivity; HFS: hemifacial spasm; HC: healthy control; REZ: root exit zone; DTI: diffusion tensor imaging.

patients, 20.00%), a vein (6 patients, 10.00%) and the vertebral artery (2 patients, 3.33%). The degree of compression was mainly grade II or III (54 patients, 90.00%). In the HC group, 8 (26.67%) cases of asymptomatic NVC were found in the unilateral cerebellopontine angle area (5 with grade I and 3 with grade II), and the anterior inferior cerebellar artery was the most common involved vessel.

Inter-group and lateral comparisons of DTI parameters

FA: Compared to both the contralateral side (0.48±0.05) and HC bilateral mean (0.49±0.04), affected-side REZ FA was significantly reduced in HFS patients (0.35±0.06, both *P*<0.001). FA values did not differ significantly between the unaffected side in HFS and HC controls (*P*=0.343). These findings indicate microstructural disruption at the affected REZ, with reduced nerve fiber organization and density.

MD: In HFS, MD on the symptomatic side (1.25±0.15×10^{-3} mm^2/s) was significantly higher than that on the contralateral side (1.05±0.10×10^{-3} mm^2/s) and in controls (1.03±0.09×10^{-3} mm^2/s), both *P*<0.001. MD values were comparable between the HFS unaffected side and HC group (*P*=0.358). The elevated MD values reflect an increase in the overall tissue diffusivity in this region and may be related to edema, tissue laxity, or gliosis.

RD: Symptomatic-side RD in HFS (0.95±0.14×10^{-3} mm^2/s) was significantly elevated compared to that on the unaffected side (0.78±0.09×10^{-3} mm^2/s) and in the HC group (0.76±0.08×10^{-3} mm^2/s), both *P*<0.001. No significant difference in RD was observed between the HFS unaffected side and controls (*P*=0.306).

AD: Although AD on the HFS affected side (1.45±0.18×10^{-3} mm^2/s) was slightly higher than that on the unaffected side (1.42±0.15×10^{-3} mm^2/s) and in controls (1.43±0.14×10^{-3} mm^2/s), the differences were not statistically significant (**Table 2**).

Comparison of the affected side in the HFS group to the asymptomatic NVC side of HC

Comparison between the affected side in the HFS group and the contact side in the 8 HC participants with asymptomatic NVC showed that the asymptomatic NVC sides exhibited higher FA (0.47±0.05) and lower MD (1.07±0.11×10^{-3} mm^2/s) and RD (0.67±0.09×10^{-3} mm^2/s) compared to the affected sides in HFS (all *P*<0.05; **Table 3**).

Diagnostic efficacy of DTI metrics

FA demonstrated the highest diagnostic accuracy for differentiating HFS from controls, with an AUC of 0.968, which was higher than that of MD (AUC=0.849) and RD (AUC=0.846). The sensitivity of FA was 86.00%, and the specificity was 98.00%. The sensitivity of MD was 76.00%, and the specificity was 84.00%. The sensitivity and specificity of RD were 72.00% and 86.00%, respectively. Detailed diagnostic efficacy measures are shown in **Table 4** and **Figure 2**.

Table 3. Comparison of DTI metrics between HFS group and HC subgroup with asymptomatic NVC

Parameter	HFS group (n=60)	HC group with asymptomatic NVC (n=8)	*t*	*P*
FA	0.35±0.06	0.47±0.05	5.402	<0.001
MD (×10^{-3} mm^2/s)	1.25±0.15	1.07±0.11	3.269	0.002
RD (×10^{-3} mm^2/s)	0.95±0.14	0.67±0.09	5.487	<0.001

Note: DTI: diffusion tensor imaging; FA: fractional anisotropy; MD: mean diffusivity; RD: radial diffusivity; HFS: hemifacial spasm; HC: healthy control; NVC: neurovascular contact.

Table 4. Diagnostic performance of DTI metrics in differentiating HFS from healthy controls

Parameter	AUC (95% CI)	Optimal cutoff	Sensitivity (%)	Specificity (%)
FA	0.968 (0.911-0.993)	0.416	86.00	98.00
MD (×10^{-3} mm^2/s)	0.849 (0.764-0.913)	1.115	76.00	84.00
RD (×10^{-3} mm^2/s)	0.846 (0.760-0.910)	0.854	72.00	86.00

Note: DTI: diffusion tensor imaging; HFS: hemifacial spasm; AUC: area under the curve; CI: confidence interval; FA: fractional anisotropy; MD: mean diffusivity; RD: radial diffusivity.

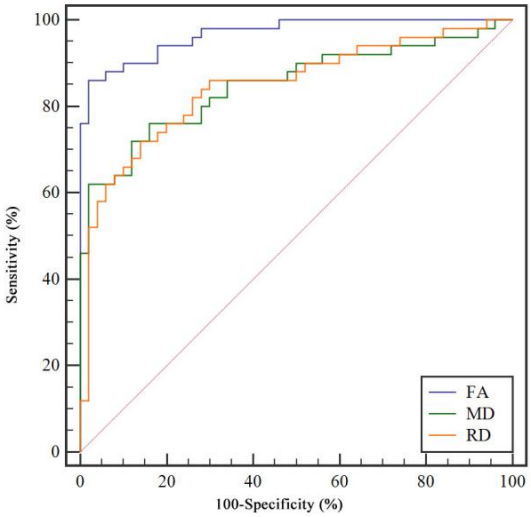

Figure 2. ROC plot of each DTI metric for differentiating HFS patients from healthy controls. Note: The area under the curve for FA was 0.968 (95% CI: 0.911-0.993), for MD was 0.849 (95% CI: 0.764-0.913), and for RD was 0.846 (95% CI: 0.760-0.910). FA: fractional anisotropy; MD: mean diffusivity; RD: radial diffusivity; ROC: receiver operating characteristic; DTI: diffusion tensor imaging; HFS: hemifacial spasm; CI: confidence interval.

Table 5. Correlations between DTI metrics on the affected side and clinical features in HFS patients

Parameter	FA	MD	RD
Disease duration	-0.452*	0.398*	0.421*
Spasm severity	-0.382*	0.287*	0.351*

Note: *P<0.05; DTI: diffusion tensor imaging; HFS: hemifacial spasm; FA: fractional anisotropy; MD: mean diffusivity; RD: radial diffusivity.

Table 6. Treatment outcomes at 6 months post-surgery

Outcome grade	Criteria	n	%
Grade I	Cured	36	60.00
Grade II	Markedly effective	19	31.67
Grade III	Effective	4	6.67
Grade IV	Ineffective	1	1.67

Correlation analysis between DTI parameters and clinical features

Affected-side FA in HFS correlated inversely with disease duration (r=-0.452, P<0.05), indicating progressive decline over time. Both MD (r=0.398) and RD (r=0.421) on the symptomatic side showed positive correlations with disease duration (both P<0.05). Regarding clinical severity, the baseline spasm severity assessed by the Cohen grade was moderately negatively correlated with FA on the affected side (r=-0.382, P<0.05) and positively correlated with RD (r=0.351, P<0.05). MD also exhibited a weak but significant positive correlation (r=0.287, P<0.05; **Table 5**).

Surgical outcomes and complications

All 60 patients were followed up for at least 6 months. The distribution of surgical outcomes at 6 months postoperatively is shown in **Table 6**. There were 55 patients (91.67%) in the good prognosis group (cured or markedly effective) and 5 patients (8.34%) in the poor prognosis group (effective or ineffective).

Table 7. Baseline characteristics and preoperative DTI metrics: good vs. poor prognosis groups

Variable	Good prognosis (n=55)	Poor prognosis (n=5)	χ^2/t	*P*
Age (years)	52.08±8.54	52.44±7.95	0.091	0.928
Sex (M/F)	24/31	2/3	0.099	0.753
Affected side (L/R)	25/30	1/4	0.395	0.530
Disease duration (years)	5.12±1.56	7.88±1.65	3.772	<0.001
FA	0.36±0.05	0.24±0.04	5.203	<0.001
MD ($\times10^{-3}$ mm^2/s)	1.27±0.13	1.33±0.12	4.123	<0.001
RD ($\times10^{-3}$ mm^2/s)	0.94±0.16	1.06±0.11	1.636	0.107
AD ($\times10^{-3}$ mm^2/s)	1.44±0.15	1.56±0.17	1.696	0.095

Note: DTI: diffusion tensor imaging; FA: fractional anisotropy; MD: mean diffusivity; RD: radial diffusivity; AD: axial diffusivity; M/F: male/female; L/R: left/right.

Table 8. Multivariate analysis of factors associated with poor prognosis after MVD

Variable	*β*	SE	Wald χ^2	*P*	OR	95% CI
Preoperative FA	-0.285	0.102	7.808	0.005	0.752	0.616-0.918
Disease duration	0.183	0.128	2.047	0.152	1.201	0.935-1.543
Preoperative MD	0.025	0.034	0.527	0.468	1.025	0.959-1.096
Constant	5.420	2.015	7.234	0.007	225.78	-

Note: SE: standard error; CI: confidence interval; OR: odds ratio; FA: fractional anisotropy; MD: mean diffusivity; MVD: microvascular decompression.

In terms of postoperative complications, a total of 5 patients (8.34%) had transient neurological dysfunction, including 3 cases of delayed facial paralysis (House-Brackmann II-III) and 2 cases of mild sensorineural hearing loss. All of these patients recovered completely within 3 months after surgery. One additional patient (1.67%) had permanent mild high-frequency hearing loss, which did not cause a significant impact on daily life.

Comparison of preoperative baseline characteristics and DTI metrics between the good prognosis and the poor prognosis groups

Compared to the good prognosis group, the preoperative FA value of the affected nerve in the poor prognosis group was significantly lower, and the MD value was significantly higher. The difference was significant ($P<0.05$). There was no significant difference in RD value or AD value between the two groups ($P>0.05$) (**Table 7**).

Multivariate logistic regression analysis

Variables with $P<0.10$ on univariate testing (disease duration, preoperative FA, and preoperative MD) were entered into a multivariate binary logistic regression model to adjust for confounding and identify independent predictors. After adjusting for other factors, preoperative FA remained an independent predictor of postoperative outcome (OR=0.752; 95% CI: 0.616-0.918; $P=0.005$; **Table 8**).

Predictive efficacy of preoperative FA for postoperative outcomes

Based on the multivariate findings, the prognostic value of preoperative FA was further assessed. Receiver operating characteristic analysis yielded an AUC of 0.780 (95% CI: 0.640-0.885) for preoperative FA in predicting poor postoperative outcome, indicating moderate discriminatory ability. Using the maximum Youden index, a preoperative FA value ≤0.378 was identified as the optimal predictive cutoff. At this cutoff, the sensitivity for predicting poor prognosis was 87.50%, and the specificity was 64.29%. Based on the prevalence of poor outcomes in our cohort (8.34%), the positive predictive value was 18.20% and the negative predictive value was 98.30%. Patients with preoperative FA >0.378 had a very high probability of achieving a good surgical outcome, which may enhance clinical confidence in surgical decision-making. To further assess the robustness of this cutoff despite the limited number of poor-outcome cases, we performed

Table 9. Predictive performance of preoperative FA

Parameter	AUC (95% CI)	Optimal cutoff	Sensitivity (%)	Specificity (%)
FA	0.780 (0.640-0.885)	0.378	87.50	64.29

Note: AUC: area under the curve; CI: confidence interval; FA: fractional anisotropy.

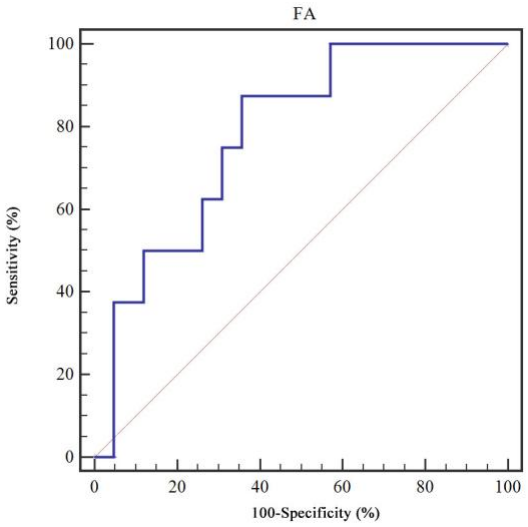

Figure 3. ROC curve of the prediction model for poor prognosis. Note: The AUC for FA was 0.780 (95% CI: 0.640-0.885), for MD was 0.849 (95% CI: 0.764-0.913), and for RD was 0.846 (95% CI: 0.760-0.910). FA: fractional anisotropy; AUC: area under the curve; ROC: receiver operating characteristic; CI: confidence interval.

bootstrap resampling with 1,000 replicates. The median cutoff value derived from the Youden index across bootstrap samples was 0.375 (interquartile range: 0.365-0.385), closely approximating the original threshold and indicating acceptable stability. Moreover, all five patients in the poor prognosis group had FA values below 0.378 (range 0.19-0.30), underscoring the consistency of this cutoff in identifying individuals at higher risk of unfavorable surgical outcomes. These findings support the clinical use of the preoperative FA threshold, even within the context of a modest sample size (**Table 9**; **Figure 3**).

Discussion

In the current study, by systematically optimizing the DTI data acquisition and post-processing methods, the microstructural changes in the REZ of patients with HFS were quantitatively analyzed, and the value of DTI metrics for the diagnosis and differentiation, disease evaluation, and prognosis prediction of MVD was evaluated. The main findings included: (1) In HFS, the affected REZ exhibited a distinct DTI profile: reduced FA, elevated MD and RD, and stable AD; (2) FA values showed excellent diagnostic efficacy in differentiating HFS patients from HCs (AUC=0.968); (3) DTI can effectively distinguish symptomatic compression from NVC; (4) Preoperative FA values were negatively correlated with disease duration and spasm severity, and served as an independent predictor of MVD efficacy (OR=0.752). These results not only provide in vivo imaging evidence for the pathophysiologic mechanism of HFS, but also signal a transition in its diagnosis and treatment strategy from macroscopic morphologic evaluation to quantitative and individualized microstructural assessment.

The results showed that the DTI technical protocol used in this study was optimized for the special challenges of small cranial nerve imaging in the posterior fossa region. By using 3.0T high-field MRI, local tilt scanning, parallel imaging technology, and high-resolution isotropic voxels (2 mm^3), the signal-to-noise ratio and spatial resolution of facial nerve REZ imaging were significantly improved while ensuring clinical feasibility, and the interference by partial volume effects and susceptibility artifacts was reduced [23]. In data processing, ROI delineation guided by multimodal image fusion (DTI parametric map and 3D-T2-weighted sequence registration) was performed independently by two blinded physicians to ensure the accuracy and repeatability of extraction of DTI metrics (ICC >0.8). This standardized process lays a methodological foundation for the precise application of DTI in cranial nerve diseases.

The DTI metrics pattern of decreased FA, increased RD, and relatively preserved AD on the affected side of HFS patients found in this study is similar to, yet distinct from, the DTI findings in patients with TN. Zhang et al. [20] found a significant decrease in FA and an increase in RD in the REZ on the affected side in classic TN, but also a decreasing trend in AD, suggesting that axonal injury and demyelination may coexist in TN. In contrast, the

absence of significant AD changes in HFS patients in the present study suggests that the pathologic injury may be predominantly demyelinating with relatively preserved axons, which is consistent with the paroxysmal and reversible characteristics of HFS clinical symptoms [24]. As a key barrier limiting the radial diffusion of water molecules, the loss of a myelin sheath will lead to an increase in RD. The decrease in FA reflects a reduced order and integrity of nerve fibers. This characteristic change is consistent with the intraoperative findings of nerve compression deformation and pathologically expected demyelination, and also explains from an imaging perspective why simple anatomical contact (asymptomatic NVC) is not sufficient to cause symptoms-only when compression results in substantial microstructural damage will abnormal electrical signal transmission and clinical symptoms occur [25, 26]. In this study, DTI metrics on the asymptomatic NVC side in the HCs were significantly different from those on the affected side of HFS (e.g., higher FA values), further confirming that DTI can look beyond gross morphology and reveal the biological effects of compression. Thus, it effectively addresses the clinical dilemma that traditional MRI can only show "contact" and cannot distinguish pathological from harmless compression [13]. Similarly, the systematic review by Liang et al. [27] also pointed out that traditional MRI has limitations in distinguishing symptomatic from asymptomatic compression, and quantitative techniques such as DTI are expected to compensate for this deficiency. As noted in the review by Jesuthasan et al. [28], the over-reporting of incidental neurovascular contacts in conventional MRI may lead to inappropriate surgical intervention, highlighting the clinical need for objective biomarkers such as DTI. Notably, the RD value in the asymptomatic NVC subgroup ($0.67\pm0.09\times10^{-3}$ mm^2/s) was lower than the bilateral mean RD of the entire HC group ($0.76\pm0.08\times10^{-3}$ mm^2/s). This may be attributable to the fact that the asymptomatic NVC subgroup represents a selected subset of healthy individuals with identifiable NVC but without clinical symptoms; their nerve microstructure may remain well preserved, resulting in diffusion parameters closer to optimal values. Alternatively, the small sample size (n=8) of this subgroup may introduce sampling variability, and this finding should be interpreted with caution.

In terms of diagnostic efficacy, FA values showed high sensitivity (86.00%) and specificity (98.00%), with an AUC of 0.968, which was significantly better than MD and RD. This suggests that FA, as a core indicator reflecting the integrity of nerve fibers, holds significant value for the auxiliary diagnosis of HFS. Particularly for cases with atypical clinical manifestations or those difficult to distinguish from other facial movement disorders, DTI quantitative analysis can serve as an objective imaging biomarker, providing a supplementary basis for diagnosis. The research conducted by Zhu et al. [29] further indicates that combining conventional DTI metrics with geometric microstructural features can improve the differentiation of HFS from other facial movement disorders such as Meige's syndrome and facial palsy, highlighting the potential of DTI-based biomarkers for differential diagnosis. DTI metrics also correlated with clinical status: FA inversely correlated with both disease duration and spasm severity (Cohen grade), whereas MD and RD showed positive associations with disease duration. Interestingly, Zhang et al. [23] reported increased FA in the superior longitudinal fasciculus of HFS patients, which positively correlated with disease duration and spasm severity. This suggests that microstructural alterations in HFS may extend beyond the REZ to involve central white matter tracts, and that FA changes in different brain regions may reflect distinct pathologic processes-peripheral demyelination at the REZ versus central reorganization or compensatory changes. This finding not only verifies the progressive characteristics of nerve injury that worsen with prolonged compression time, but also indicates that DTI metrics are likely to become an objective tool to quantify disease severity, moving beyond subjective symptom descriptions and assisting in clinical hierarchical management [30].

A key contribution of this work was establishing preoperative DTI metrics as prognostic indicators for MVD outcomes. Multivariable regression identified preoperative affected-side FA as an independent determinant of 6-month postoperative outcomes, and its predictive efficiency was above medium (AUC=0.780). When FA value ≤0.378, the sensitivity of predicting poor prognosis was 87.50%. This finding aligns with a systematic review by Cipollina et al. [31] demonstrating that preoperative FA and RD predict

outcomes after MVD for TN. However, while lower FA was associated with better outcomes in that review, our study found that higher FA predicted favorable prognosis-a discrepancy that may reflect differences in the pathophysiology of sensory versus motor cranial nerves. This suggests that the severity of preoperative nerve microstructural injury directly determines the potential for postoperative nerve repair and the upper limit of functional recovery. For patients with low FA values, surgeons can conduct more thorough risk assessment and doctor-patient communication before surgery, implement more refined decompression procedures during surgery, and formulate individualized rehabilitation plans after surgery, thereby optimizing the overall treatment strategy [32]. At the same time, the dynamic changes in DTI metrics after surgery (such as increased FA and decreased RD in the good prognosis group) provide visual imaging evidence of the nerve repair process (e.g., remyelination), making DTI a useful tool for monitoring surgical effects and biological response. This is consistent with findings from Jin et al. [33], who reported that FA values in HFS patients increased significantly at 6 months and 1 year after MVD compared to preoperative values, while apparent diffusion coefficient values decreased. Furthermore, animal studies have demonstrated that DTI can detect axonal regeneration and remyelination following nerve injury, with FA increasing and RD decreasing as nerves recover [34, 35]. These observations support the interpretation that postoperative DTI changes in HFS patients reflect genuine neurobiological recovery processes.

This study still has several limitations: (1) As a single-center study with a relatively modest sample size-particularly only five patients (8.34%) in the poor prognosis group-the statistical power of the multivariable analysis was limited, and the estimated odds ratios may be subject to small-sample bias. Although Firth's penalized likelihood method was employed to mitigate this issue, the findings require confirmation in larger, multicenter cohorts. The generalizability of our predictive model is therefore preliminary. Of note, although the small sample size may introduce instability in the estimation of mean values, all five patients in the poor prognosis group had FA values below the cutoff of 0.378, supporting the consistency of the observed association between lower FA and poorer outcome. (2) Although manual ROI segmentation has been standardized and demonstrates high consistency, it still involves subjectivity. Automated or semi-automated segmentation algorithms could be explored in the future to improve efficiency. (3) As an indirect measurement, DTI cannot accurately distinguish the contributions of different pathologic processes such as demyelination, axonal injury, and gliosis. DTI combined with more advanced diffusion models (e.g., neurite orientation dispersion and density imaging) may provide more specific information. (4) The follow-up time was short (6 months), and the long-term recurrence rate and long-term evolution of DTI metrics could not be observed. Further research should focus on: (1) Establishing standardized DTI scanning and post-processing protocols across centers to promote the widespread application of DTI technology; (2) Constructing a multimodal prediction model integrating DTI metrics, clinical indicators, conventional MRI findings, and electrophysiological measures, along with machine learning approaches, to enhance prognostic precision; (3) Conducting longitudinal studies to clarify the dynamic changes of DTI metrics at different time points after surgery and their relationship with the improvement of clinical symptoms; (4) Expanding the application of DTI in the study of central remodeling mechanisms, and comprehensively revealing the "peripheral-central" network interaction mechanism of HFS in combination with functional MRI and other technologies [36-38].

Conclusion

This work provides comprehensive evidence supporting the diagnostic and therapeutic utility of DTI in HFS. By optimizing the data acquisition and post-processing procedures, DTI can noninvasively and quantitatively reveal the characteristic microstructural damage of the REZ in patients, which in manifested as decreased FA and increased RD, providing *in vivo* imaging evidence for the pathological hypothesis of demyelination caused by neurovascular compression. DTI not only demonstrates excellent diagnostic efficacy, effectively distinguishing between pathological compression and asymptomatic contact, but its metrics are also correlated with disease duration and

symptom severity, serving as a tool for quantitative disease evaluation. More importantly, preoperative FA value is an independent and reliable biomarker for predicting the long-term efficacy of MVD, providing an objective basis for individualized prognosis assessment and clinical decision-making. The integration of DTI into the preoperative evaluation system for HFS marks a new era in the diagnosis and treatment model-shifting from reliance on macroscopic morphological experience to integrating microstructural quantitative information for precision and individualization. Although challenges remain in standardization and technical optimization, DTI has undoubtedly become a key bridge to advancing the development of precision diagnosis and treatment for cranial nerve diseases.

Disclosure of conflict of interest

None.

Address correspondence to: Fangang Meng, Beijing Neurosurgical Institute, Beijing Tiantan Hospital, Capital Medical University, No. 119, South Fourth Ring West Road, Fengtai District, Beijing 100070, China. E-mail: fgmeng@ccmu.edu.cn

References

[1] Son BC, Ko HC and Choi JG. Hemifacial spasm caused by vascular compression in the cisternal portion of the facial nerve: report of two cases with review of the literature. Case Rep Neurol Med 2019; 2019: 8526157.

[2] Wang J, Chong Y, Jiang C, Dai Y, Liang W and Ding L. Microvascular decompression for hemifacial spasm involving the vertebral artery. Acta Neurochir (Wien) 2022; 164: 827-832.

[3] Mizobuchi Y and Nagahiro S. Prevalences of trigeminal neuralgia and hemifacial spasm. No Shinkei Geka 2024; 52: 22-28.

[4] Lee JA, Han YK, Jung WJ, Lee BH and Lee S. Personality traits and their effects in patients with hemifacial spasm. Sci Rep 2025; 15: 12209.

[5] Duan Y, Lv K, Zhao C, Han L, Wang J, Zhang C, Zhang Z, Liu H, Yang K, Yuan Z, Zhu L, Wang Y, Luan J, Ma G and Liu J. Exploring facial nucleus-centered connectivity in hemifacial spasm: novel insights into pathogenesis and surgical impact. Brain Topogr 2025; 38: 58.

[6] Ma T, Zhang X, Wu J, Fan S and Wang W. Research progress of acupuncture and moxibustion in treating peripheral facial paralysis. Integrative Medicine and Nursing Advances 2025; 1: 1-7.

[7] Zhao K, Wang J, Liu W, Zhang J, Shu K and Lei T. Flat-shaped posterior cranial fossa was associated with poor outcomes of microvascular decompression for primary hemifacial spasm. Acta Neurochir (Wien) 2020; 162: 2801-2809.

[8] Rhomberg T, Eördögh M, Lehmann S and Schroeder HWS. Endoscope-assisted microvascular decompression in hemifacial spasm with a teflon bridge. Acta Neurochir (Wien) 2024; 166: 239.

[9] Liu Y, Liu L, Wang J, Ge S and Qu Y. An unusual abnormal muscular response during microvascular decompression under endoscope assistance. J Craniofac Surg 2022; 33: e390-e392.

[10] Wu F, Wei HN, Zhang M, Ma QF, Li R and Lu J. High-resolution magnetic resonance imaging radiomics for identifying high-risk intracranial plaques. Transl Stroke Res 2025; 16: 1745-1755.

[11] Kim J, Na I, Chung J, Song HN, Kim K, Ju S, Eun MY, Seo WK and Park H. Enhancing intracranial vessel segmentation using diffusion models without manual annotation for 3D Time-of-Flight Magnetic Resonance Angiography. Comput Med Imaging Graph 2025; 125: 102651.

[12] Miller JP, Acar F, Hamilton BE and Burchiel KJ. Radiographic evaluation of trigeminal neurovascular compression in patients with and without trigeminal neuralgia. J Neurosurg 2009; 110: 627-632.

[13] Traylor KS, Sekula RF, Eubanks K, Muthiah N, Chang YF and Hughes MA. Prevalence and severity of neurovascular compression in hemifacial spasm patients. Brain 2021; 144: 1482-1487.

[14] Tohyama S, Walker MR, Sammartino F, Krishna V and Hodaie M. The utility of diffusion tensor imaging in neuromodulation: moving beyond conventional magnetic resonance imaging. Neuromodulation 2020; 23: 427-435.

[15] Jerome NP, Caroli A and Ljimani A. Renal diffusion-weighted imaging (DWI) for apparent diffusion coefficient (ADC), intravoxel incoherent motion (IVIM), and diffusion tensor imaging (DTI): basic concepts. Methods Mol Biol 2021; 2216: 187-204.

[16] Lope-Piedrafita S. Diffusion tensor imaging (DTI). Methods Mol Biol 2018; 1718: 103-116.

[17] Boucher S, Arribarat G, Cartiaux B, Lallemand EA, Péran P, Deviers A and Mogicato G. Diffusion tensor imaging tractography of white matter tracts in the equine brain. Front Vet Sci 2020; 7: 382.

[18] Boss MA, Malyarenko D, Partridge S, Obuchowski N, Shukla-Dave A, Winfield JM, Fuller CD, Miller K, Mishra V, Ohliger M, Wilmes LJ, Attariwala R, Andrews T, deSouza NM, Margolis DJ and Chenevert TL. The QIBA profile for diffusion-weighted MRI: apparent diffusion coeffi-

cient as a quantitative imaging biomarker. Radiology 2024; 313: e233055.
[19] Geraldo AF, Pereira J, Nunes P, Reimão S, Sousa R, Castelo-Branco M, Pinto S, Campos JG and de Carvalho M. Beyond fractional anisotropy in amyotrophic lateral sclerosis: the value of mean, axial, and radial diffusivity and its correlation with electrophysiological conductivity changes. Neuroradiology 2018; 60: 505-515.
[20] Zhang Y, Mao Z, Cui Z, Ling Z, Pan L, Liu X, Zhang J and Yu X. Diffusion tensor imaging of axonal and myelin changes in classical trigeminal neuralgia. World Neurosurg 2018; 112: e597-e607.
[21] Halawani AM, Tohyama S, Hung PS, Behan B, Bernstein M, Kalia S, Zadeh G, Cusimano M, Schwartz M, Gentili F, Mikulis DJ, Laperriere NJ and Hodaie M. Correlation between cranial nerve microstructural characteristics and vestibular schwannoma tumor volume. AJNR Am J Neuroradiol 2021; 42: 1853-1858.
[22] Seo Y, Rollins NK and Wang ZJ. Reduction of bias in the evaluation of fractional anisotropy and mean diffusivity in magnetic resonance diffusion tensor imaging using region-of-interest methodology. Sci Rep 2019; 9: 13095.
[23] Zhang J, Yu Q, Gu P, Sun H, Yuan F and Zhang Q. Brain structure alterations in hemifacial spasm: a diffusion tensor imaging study. Clin EEG Neurosci 2022; 53: 165-172.
[24] Wang Y, Wang D, Wu Y, Zhu C, Wei W, Li Y, Li L, Chen W and Chen M. A preliminary study of diffusion tensor imaging in root entry zone of primary trigeminal neuralgia. Front Neuroanat 2023; 17: 1112662.
[25] Al Menabbawy A, Al Mutawa M, Tran V, Lehmann S, El Refaee E, Matthes M and Schroeder HWS. The impact of perforating arterial branches on microvascular decompression for hemifacial spasm. Neurosurg Focus 2025; 59: E3.
[26] Zhang T, Zhao C, Qi X, Li R, Liu Y and Chen F. Brain white matter structural alteration in hemifacial spasm: a diffusion tensor imaging study. J Craniofac Surg 2023; 34: 674-679.
[27] Liang C, Yang L, Reichardt W, Zhang B and Li R. Different MRI-based methods for the diagnosis of neurovascular compression in trigeminal neuralgia or hemifacial spasm: a network meta-analysis. J Clin Neurosci 2023; 108: 19-24.
[28] Jesuthasan A, Natalwala A, Davagnanam I, Saifee T and Zrinzo L. Hemifacial spasm: an update on pathophysiology, investigations and management. J Neurol 2025; 272: 502.
[29] Zhu H, Yang A, Luan J, Xu M, Liu B, Lv K, Hu P, Shmuel A, Zhu H, Yuan Z, Shu N, Cheng J and Ma G. Geometric microstructural characteristics of white matter differentiate patients with facial dyskinesias and palsy. CNS Neurosci Ther 2026; 32: e70733.
[30] Guo C, Xu H, Niu X, Krimmel S, Liu J, Gao L, Zhang M and Wang Y. Abnormal brain white matter in patients with hemifacial spasm: a diffusion tensor imaging study. Neuroradiology 2020; 62: 369-375.
[31] Cipollina GP, Costanzo R, Campisi BM, Scalia G, Brunasso L, Bonosi L, Iacopino DG and Maugeri R. Pre-treatment DTI markers: predicting clinical outcomes in microvascular decompression for classic trigeminal neuralgia - a systematic review. Neurosurg Rev 2024; 47: 833.
[32] Fang L, Haidong S, Jianfeng L and Ruen L. Analysing correlation between the facial nerve notch at the root exit zone and long-term effect in patients with hemifacial spasm after microvascular decompression: a prospective study. Neurol India 2022; 70: 1819-1823.
[33] Jin Z and Li Z. Clinical application of diffusion tensor imaging in diagnosis and prognosis of hemifacial spasm. World Neurosurg 2021; 145: e14-e20.
[34] Manzanera Esteve IV, Farinas AF, Pollins AC, Nussenbaum ME, Cardwell NL, Kang H, Does MD, Thayer WP and Dortch RD. Probabilistic assessment of nerve regeneration with diffusion MRI in rat models of peripheral nerve trauma. Sci Rep 2019; 9: 19686.
[35] Paul DA, Gaffin-Cahn E, Hintz EB, Adeclat GJ, Zhu T, Williams ZR, Vates GE and Mahon BZ. White matter changes linked to visual recovery after nerve decompression. Sci Transl Med 2014; 6: 266ra173.
[36] Tu Y, Yu T, Wei Y, Sun K, Zhao W and Yu B. Structural brain alterations in hemifacial spasm: a voxel-based morphometry and diffusion tensor imaging study. Clin Neurophysiol 2016; 127: 1470-1474.
[37] Yu Q, Cui Y, Dong S, Ma Y, Xiao Y, Fan L and Liu S. Altered brain structure in hemifacial spasm patients: a multimodal brain structure study. Int J Gen Med 2024; 17: 4435-4443.
[38] Maguire EA, Spiers HJ, Good CD, Hartley T, Frackowiak RS and Burgess N. Navigation expertise and the human hippocampus: a structural brain imaging analysis. Hippocampus 2003; 13: 250-259.